Available online at www.sciencedirect.com
ScienceDirect
Journal of Molecular Catalysis A: Chemical 272 (2007) 136–141
JOURNAL OF MOLECULAR CATALYSIS A: CHEMICAL
www.elsevier.com/locate/molcata

One-step synthesis of palladium/SBA-15 nanocomposites and its catalytic application

Peng Han [a,b], Xiaomei Wang [a,b], Xuepeng Qiu [b], Xiangling Ji [a,*], Lianxun Gao [a,b,*]

[a] State Key Laboratory of Polymer Physics and Chemistry, Changchun Institute of Applied Chemistry, Chinese Academy of Sciences, Graduate School of the Chinese Academy of Sciences, 5625 Renmin Street, Changchun 130022, People's Republic of China
[b] Laboratory of Polymer Engineering, Changchun Institute of Applied Chemistry, Chinese Academy of Sciences, Graduate School of the Chinese Academy of Sciences, 5625 Renmin Street, Changchun 130022, People's Republic of China

Received 7 November 2006; received in revised form 1 March 2007; accepted 2 March 2007
Available online 12 March 2007

Abstract

Well-dispersed palladium nanoparticles in mesoporous SBA-15 SiO_2 were prepared in a facile one-step approach during sol–gel route under reductive atmosphere. X-ray diffraction (XRD) results indicate that as-synthesized nanocomposites basically remain ordered two-dimensional hexagonal mesostructure while transmission electron microscopy (TEM) study exhibits a well dispersion of palladium nanoparticles within the mesoporous SBA-15 channels. The size of Pd nanoparticles is approximately in the range of 5–10 nm. However, the resulting nanocomposites exhibit a highly catalytic activity and reused ability at least after five recycles without ligand in air for both the Suzuki and Heck coupling reactions.

Keywords: Mesoporous SBA-15; Palladium nanoparticles; Suzuki coupling reaction; Heck coupling reaction

1. Introduction

Metal nanoparticles exhibit unique properties on optical, electronic and chemical behavior which is quite different from bulk metal materials due to quantum size effect, surface effect and others effects [1–3]. Transition metal nanoparticles as good catalysts for organic synthesis have attracted much attention over the past decade [4–7]. But the liquid suspensions of metal nanoparticles in catalysis will bring some problems such as in recycle and the separation of the catalyst from reaction system. Thus, some work focused on immobilizing metal nanoparticles on suitable support materials. Actually, many immobilization methods and support materials have been reported in literature [8–11]. However, inorganic solids such as charcoal, silica, Al_2O_3, TiO_2 or MgO are widely exploited to carry some metal nanoparticles.

Palladium as catalyst plays an important role in organic synthesis [12–17]. Zero valence palladium exhibits good catalytic activity in C–C bond formation [18–20]. But there is an obvious problem for the recycle of palladium in large-scale application. Thus, it is necessary to develop new-type heterogeneous catalysts which can be recovered from the reaction system readily and recycled usage. Since mesoporous silicates possess lager surface area, uniform pore structure and inert environment for immobilization of transition metal nanoparticles [21], it has become an excellent carrier for many functional materials. For example, Pd nanoparticles as catalyst were introduced in mesoporous silica [22–29] via ion exchange, wetness impregnation, chemical vapor infiltration, in situ reduction and so on. Definitely, palladium composites showed relatively high catalytic activity in the Suzuki-, Heck-, Sonogashira-, still-coupling reaction [30–41]; hydrogenation reaction [42–43] and oxidation reaction [44]. Traditional method such as ion exchange or wetness impregnation have the disadvantages of distribution unevenly or low supporting content for palladium nanoparticles [29]. Mehert et al. reported that mesoporous SiO_2 with highly dispersed Pd was made by chemical vapor infiltration and used for Heck coupling reaction with good catalytic activity [34]. However, synthesis of such a material needs complicated equipment and the suitable precursors are limited in terms of high

* Corresponding authors. Tel.: +86 431 526 2876/2203; fax: +86 431 568 5653.
E-mail addresses: xlji@ciac.jl.cn (X. Ji), lxgao@ciac.jl.cn (L. Gao).

1381-1169/$ – see front matter © 2007 Elsevier B.V. All rights reserved.
doi:10.1016/j.molcata.2007.03.006

volatility and thermal stability. Li et al. studied the mesoporous SBA-15 with high dispersion of Pd nanoparticles in the form of an ultra-thin colloid layer through in situ reduction method and the resultant composites exhibit excellent catalytic activity for activated aryl bromides with olefin in Heck carbon–carbon coupling reactions in air [35]. Papp et al. reported that Pd/MCM-41 were generated via simultaneous self-assembly of mesoporous MCM-41 silica and palladium nanoparticles generation and used for Heck coupling reaction with good catalytic activity and recycle ability. But the preparation procedure cannot control the size of Pd nanoparticles readily [33]. Hampsey et al. reported that mesoporous silica particles with palladium nanoparticles incorporated into the pore frame work have been synthesized using an aerosol-assisted self assembly process and used in the hydrodechlorination reaction of 1,2-dichloroethane [30].

Herein, we present a facile one-step method to prepare palladium nanoparticles/SBA-15 through sol–gel reaction. SBA-15 SiO_2 has pore size in the range of 5–10 nm, large specific surface area and highly ordered pore structure [45]. The loading amount of palladium nanoparticles in SBA-15 was adjusted via different amount of palladium salts. Finally, the catalytic activity and recycling ability of nanocomposites was studied in the Suzuki and Heck coupling reactions.

2. Experimental

2.1. One-step synthesis on Pd/SBA-15 nanocomposites

A typical preparation of Pd/ SBA-15 nanocomposites was described in the following. For example, 1.5 g of triblock copolymer Pluronic P123 was dissolved in a solution of 11.5 mL of deionized water, 24 g of 2 M HCl and a fixed amount of (0, 0.03, 0.1, 0.2, 0.4 g) $PdCl_2$ at 35 °C under stirring, then 3.5 g of TEOS was added into the above solution. The resulting mixture was stirred moderately under H_2 atmosphere at 35 °C for 24 h, and then aged at 80 °C for 24 h under H_2 atmosphere without stirring. The polymer template P123 was removed by calcination at 450 °C for 2 h. After filtration and drying, the dark blue powder samples were available. Then, 0.5 g sample was reduced under H_2 atmosphere at 80 °C for 0.5 h. Finally, the grey powder was obtained.

2.2. Characterization

X-ray diffraction (XRD) patterns were recorded on a Rigaku D/MAX-2500 using Cu Kα radiation at 50 kV and 250 mA. Typically, the data of low-angle XRD patterns were collected in the range of $0.5° < 2\theta < 5°$ with a step size of 0.02° and a count time of 1 s per step. The data of wide-angle XRD patterns were collected in the range of $30° < 2\theta < 90°$ with a step size of 0.02° and a count time of 0.15 s per step. Transmission electron microscope (TEM) images were taken with a JEOL 1011 electron microscope with an accelerating voltage of 100 kV. The samples were prepared by dispersing the powder samples directly on copper grids. Nitrogen adsorption–desorption isotherms at 77 K for mesoporous samples were obtained using a micromeritics ASAP 2010. The specific surface area is calculated by the Brunauer–Emmett–Teller (BET) method while the pore size is obtained from the Barrett–Joyner–Halenda (BJH) model.

2.3. Catalytic reactions

A typical experiment for the Suzuki coupling reaction was carried out in a 50 mL round-bottomed flask with 20 mL of $EtOH/H_2O$ (v/v = 1:3) cosolvent using 2.0 mmol *p*-bromoacephone, 2.5 mmol of phenylboronic acid, 6.0 mmol of K_2CO_3 in the presence of 5.7 wt% Pd/SBA-15 (Pd:bromoacephone = 1:200 in molar ratio). After stirring at 85 °C for 5 h, the mixture was extracted with ethyl ether and then filtrated for recovering of catalyst. Yield was determined by gas chromatograph (GC) and ^{1}H NMR analyses. The catalysts were filtered and washed with 10 mL of dichloromethane and 10 mL of ethanol three times, respectively, and dried for next run.

A typical experiment for the Heck coupling reaction was performed in a round-bottomed flask with 10 mmol iodobenzene, 12 mmol methyl acrylate, 15 mmol triethylamine, 7.4 mg as-prepared Pd/SBA-15 (5.7 wt%) (Pd:iodobenzene = 1:1000 in molar ratio) and 20 mL NMP. After refluxing at 140 °C for 1 h, the mixture was filtrated for recovering of catalyst. The products were analyzed by the gas chromatograph and ^{1}H NMR. The recovering catalyst was washed with 10 mL of dichloromethane and 10 mL of ethanol three times, respectively, and dried for next run.

3. Results and discussion

3.1. Structure and morphology

Structure and morphology are studied by X-ray diffraction and transmission electron microscopy. Fig. 1a presents the low-angle XRD patterns for Pd/SBA-15 nanocomposites with different Pd loading. Almost all samples exhibit one intense peak at 0.86–0.98° along with two weak peaks at 1.5–1.66° and 1.74–1.9°, which correspond to 1 0 0, 1 1 0 and 2 0 0 reflections, respectively. Fig. 1b shows clear details for 1 1 0, 2 0 0 reflections. The pure SBA-15 shows a diffraction peak at a 2θ of 0.86° which corresponds to its *d*-spacing of 10.3 nm. Increasing the Pd loading leads to a decrease in *d*-spacing of 1 0 0 plane to 9.8, 9.0, 9.0 and 9.0 nm corresponding to 1.5, 5.7, 11.6 and 19.7 wt% of Pd nanoparticle samples. Fig. 2 is a TEM image of the Pd/SBA-15 nanocomposite recorded along (1 0 0) and (1 1 0) reflection. Combined XRD data with TEM images in Fig. 2, we confirmed the composites with two-dimensional hexagonal structure (*P6mm*).

Fig. 3 shows the wide-angle XRD patterns of Pd/SBA-15 nanocomposites. The typical palladium *fcc* crystalline structures can be found while the peak intensity increases with the Pd loading. According to Scherrer equation, we calculate the average Pd particles size to be approximately 10 nm from (1 1 1) plane. The average Pd particles size in Fig. 2 that we measured is 7.6 ± 1.4 nm for 5.7 wt% Pd/SBA-15 and 9.5 ± 1.6 nm for 11.6 wt% Pd/SBA-15 nanocomposites. The palladium nanoparticles were confined in the hexagonal channels of SBA-15. The uniform dispersion of Pd nanoparticles is due to homoge-

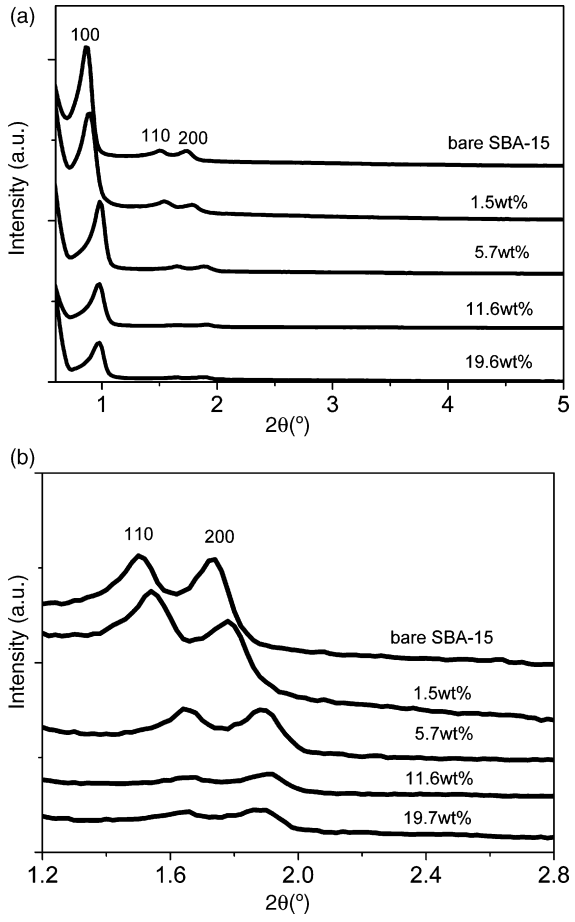

Fig. 1. Low-angle X-ray diffraction patterns for Pd/SBA-15 nanocomposites (a) and the local magnification of low-angle X-ray diffraction patterns for Pd/SBA-15 (b).

neous distribution of palladium salts into silica precursors. Fig. 4 exhibits the XRD patterns of samples with and without template. Definitely, the calcination results in formation of Pd and partial PdO nanoparticles. The content of palladium in the samples is testified finally by inductively coupled plasma-atomic emission spectroscopy (ICP-AES) elemental analysis.

The nitrogen adsorption–desorption isotherms at 77 K for samples are shown in Fig. 5a and the corresponding pore size distribution curves can be seen in Fig. 5b. These mesoporous materials exhibit a narrow pore size distribution. The Brunauer–Emmett–Teller surface area for Pd/SBA-15 nanocomposites decreases from 679 to 615, 521, 517 m^2/g with different palladium loading meanwhile the pore size decreases from 58.3 to 55.1 Å (see Table 1). Definitely, the pore volume also decreases from 0.72 to 0.48 for 1.5 wt% Pd and 19.7 wt% Pd samples. The above results are due to Pd loading in pore channels as shown in Fig. 2.

3.2. Catalytic application

3.2.1. Suzuki coupling reaction

Firstly, Suzuki coupling reaction is applied to test catalytic effect. Suzuki coupling reaction between a series of aryl bromides and aryl boronic acids was performed with both activated

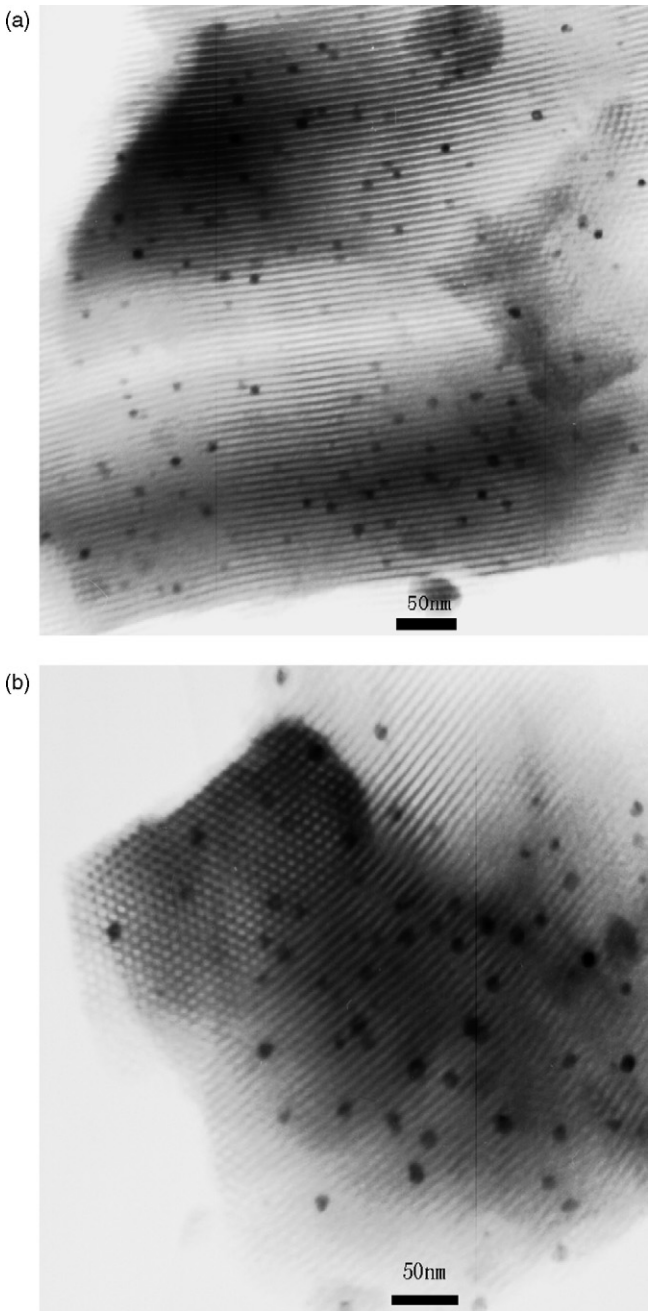

Fig. 2. TEM images for nanocomposites with different Pd loading: (a) 5.7 wt% and (b) 11.6 wt%.

Table 1
BET results

	Pd loading (wt%)			
	1.5	5.7	11.6	19.7
Surface area (m^2/g)[a]	679	615	521	517
Pore volume (cm^3/g)[b]	0.72	0.69	0.50	0.48
Average pore size (Å)[c]	58.3	57.9	56.9	55.1

[a] BET surface area.
[b] Single-point pore volume.
[c] BJH average pore diameter.

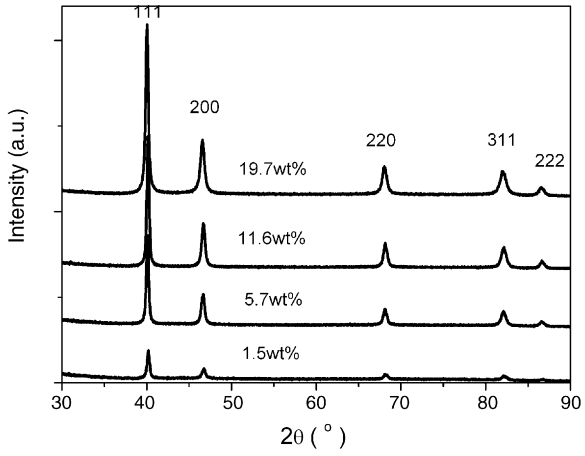

Fig. 3. XRD patterns for Pd/SBA-15 nanocomposites, the Pd loading as indicated.

and deactivated aryl bromides and they show a good yield of 80–99% as listed in Table 2. Deactivated aryl bromides have lower yield of 80–85% for entries 3–4 than activated aryl bromides for entries 1–2 with yield of 95–99% under the same conditions. So the reaction time needs to be prolonged for entries 3 and 4.

To determine the efficacy of palladium nanocomposites, we then investigated their recycle. However, the Suzuki coupling of

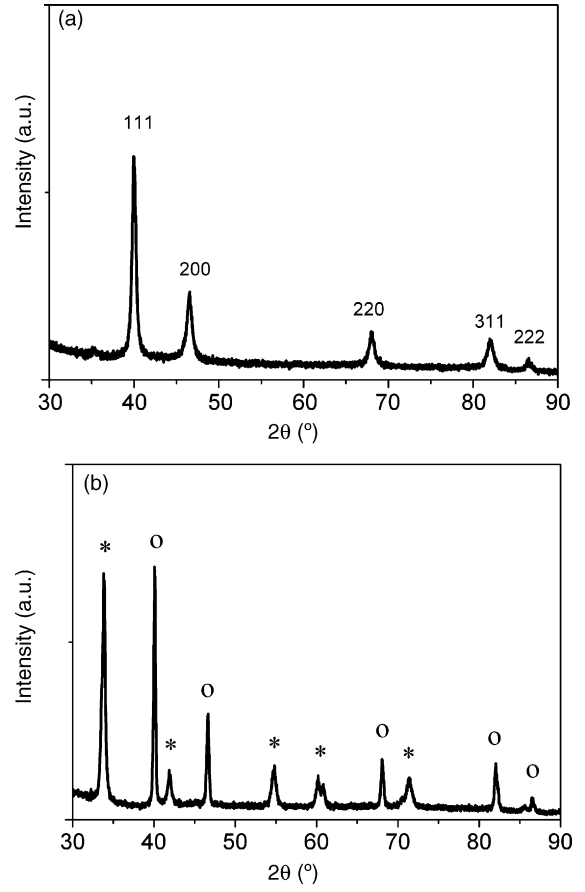

Fig. 4. XRD patterns of 5.7 wt% nanocomposites before (a) and after (b) calcinations; *, corresponding to PdO; O, corresponding to Pd.

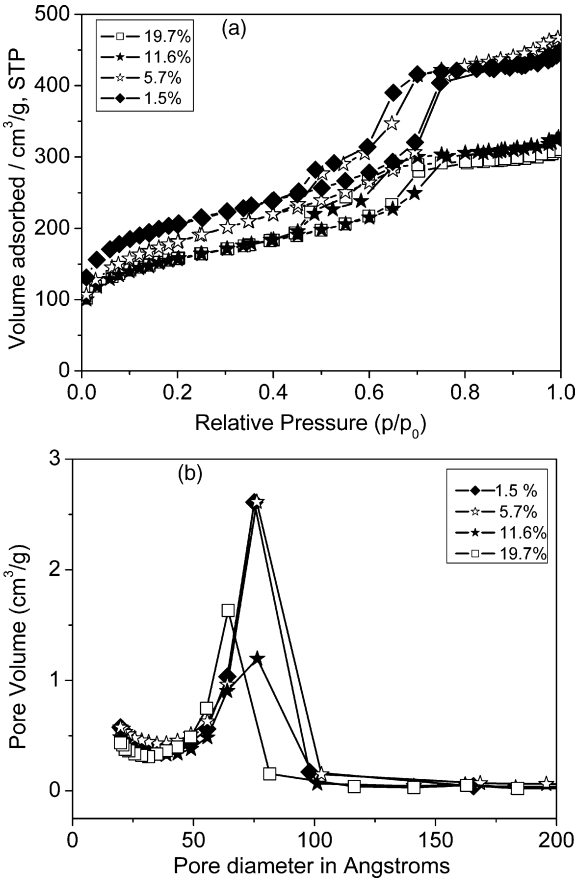

Figure 5. (a) Nitrogen adsorption–desorption isotherms for Pd/SBA-15 nanocomposites with different palladium loading and (b) corresponding pore size distribution by BJH model.

Table 2
Catalytic data for Suzuki coupling reactions

Entry	ArBr	*t* (h)	Pd (mol%)	Isolated yield (%)	TON
1	R = CH_3CO	5	0.2	99	495
2	R = NO_2	5	0.2	93	465
3	R = CH_3O	10	0.2	85	425
4	R = H	10	0.2	88	440

p-bromoacephone and phenylboronic acid exhibits high yield at least up to 95% until fifth recycling usage as shown in Table 3.

3.2.2. *Heck coupling reaction*

The second reaction system is the Heck reaction. Definitely, Heck reaction is widely used in C–C coupling. Coupling of aryl halide with olefin was carried out under optimal conditions. As listed in Table 4, coupling of aryl iodides with olefin give relatively high turn over numbers (TON) of 2000–2500 for entries

Table 3
Recycling test for Suzuki coupling reactions

Run	1	2	3	4	5
React time (h)	4	4	4	4	4
Yield (%)	99	99	95	99	98

Table 4
Reaction conditions and catalytic effect for the Heck coupling reactions

Entry	R	X	Vinyl substrate	Pd (mol%)	T (°C)	t (h)	Conversion (%) (selection (%))	TON
1	H	I	Methyl acrylate	0.04	140	1	99	2500
2	H	I	Styrene	0.04	140	3	99 (trans:cis = 84:16)	2100
3	CH_3	I	Methyl acrylate	0.04	140	3	99	2500
4	CH_3	I	Styrene	0.04	140	10	95 (trans:cis = 88:12)	2000
5	CH_3CO	Br	Methyl acrylate	0.2	140	4	95	480
6	CH_3CO	Br	Styrene	0.2	140	8	90	450

Table 5
Recycling test for Heck coupling reactions

Run	1	2	3	4	5	6
React time (h)	1	1	1	1	1	1
Yield (%)	99	98	99	95	90	70

1–4. The coupling reaction gives only trans-isomer for methyl acrylate for entries 1, 3 and 5. The coupling reaction for styrene gives trans:cis = 84:16 with iodobenzene and trans:cis = 88:12 with *p*-iodotoluene. The coupling reaction for styrene with *p*-bromoacephone gives only trans-isomer. The coupling reaction for activated aryl bromides can be fulfilled with relatively high amount Pd nanocomposites for entries 5 and 6. As shown in Table 5, this Heck coupling of iodobenzene and methyl acrylate exhibits high yield at least up to 90% until fifth recycling usage. But the yield drops to 70% in the sixth recycling which possibly comes from a leakage of palladium nanoparticles from SBA-15 channels.

4. Conclusions

A facile one-step method has been developed to synthesize the palladium nanoparticles in highly ordered mesoporous channels of SBA-15 SiO_2. The loading amount of palladium can be controlled readily. TEM images indicate the palladium nanoparticles with relatively narrow size distribution dispersed into the hexagonal pore channels homogeneously. The Pd loading results in the decrease of surface area, pore volume and average pore size. The resulting Pd/SBA-15 nanocomposites exhibit a high catalytic activity and better recycling effect at least for fifth recycle for both the Suzuki and Heck coupling reactions.

Acknowledgements

We are grateful for the support for this study provided by the National Natural Science Foundation of China (90101001, 20674085), the Distinguished Young Fund of Jilin Province (20050104), the Chinese Academy of Sciences (KJCX2-SW-H07), the International Collaboration Project (04-03GH268, 20050702-2) from Changchun City and Jilin Province, China.

References

[1] G. Schmid, M. Bäumle, M. Geerkens, I. Heim, C. Osemann, T. Sawitowski, Chem. Soc. Rev. 28 (1999) 179–185.
[2] C.N.R. Rao, A.K. Cheetham, J. Mater. Chem. 11 (2001) 2887–2894.
[3] M.-C. Daniel, D. Astruc, Chem. Rev. 104 (2004) 293–346.
[4] J. Schulz, A. Roucoux, H. Patin, Chem. Rev. 102 (2002) 3757–3778.
[5] D. Astruc, F. Lu, J.R. Aranzaes, Angew. Chem. Int. Ed. 44 (2005) 7852–7872.
[6] F. Raimondi, G.G. Scherer, R. Kötz, A. Wokaun, Angew. Chem. Int. Ed. 44 (2005) 2190–2209.
[7] M. Moreno-Manas, R. Pleixats, Acc. Chem. Res. 36 (2003) 638–643.
[8] C.M. Yang, H.S. Sheu, K.J. Chao, Adv. Funct. Mater. 12 (2002) 143–148.
[9] R. Raja, G. Sankar, S. Hermann, D.S. Shephard, S. Bromley, J.M. Thomas, B.F.G. Johnson, Chem. Commun. (1999) 1571–1572.
[10] Y.J. Han, J.M. Kim, G.D. Stucky, Chem. Mater. 12 (2000) 2068–2069.
[11] K.B. Lee, S.M. Lee, J. Cheon, Adv. Mater. 13 (2001) 517–520.
[12] Y. Uozumi, R. Nako, Angew. Chem. Int. Ed. 42 (2003) 194–197.
[13] R. Nakao, H. Rhee, Y. Uozumi, Org. Lett. 7 (2005) 163–165.
[14] R. Akiyama, S. Kobayashi, Angew. Chem. Int. Ed. 40 (2001) 3469–3471.
[15] A.M. Jansson, M. Groti, K.M. Halkes, M. Meldal, Org. Lett. 4 (2002) 27–30.
[16] C. Ramarao, S.V. Ley, C.S. Smith, I.M. Shirley, N. DeAlmeida, Chem. Commun. (2002) 1132–1133.
[17] C.K.Y. Lee, A.B. Holmes, S.V. Ley, I.F. McConvey, B. Al-Duri, G.A. Leeke, R.C.D. Santos, J.P.K. Seville, Chem. Commun. (2005) 2175–2177.
[18] E.-I. Negishi, Handbook of Organopalladium Chemistry for Organic Synthesis, John Wiley & Sons, New York, 2002.
[19] R. Narayanan, M.A. El-Sayed, J. Am. Chem. Soc. 125 (2003) 8340–8347.
[20] R. Narayanan, M.A. El-Sayed, J. Phys. Chem. B 108 (2004) 8572–8580.
[21] D.E. De Vos, M. Dams, B.F. Sels, P.A. Jacobs, Chem. Rev. 102 (2002) 3615–3640.
[22] A. Corma, Chem. Rev. 97 (1997) 2373–2420.
[23] J.Y. Ying, C.P. Mehnert, M.S. Wong, Angew. Chem. Int. Ed. 38 (1999) 56–77.
[24] H. Kang, Y.W. Jun, J.I. Park, K.B. Lee, J. Cheon, Chem. Mater. 12 (2000) 3530–3532.
[25] R.M. Rioux, H. Song, J.D. Hoefelmeyer, P. Yang, G.A. Somorjai, J. Phys. Chem. B 109 (2005) 2192–2202.
[26] V. Hornebecq, M. Antonietti, T. Cardinal, M. Treguer-Delapierre, Chem. Mater. 15 (2003) 1993–1999.
[27] V. Hulea, D. Brunel, A. Galarneau, K. Philippot, B. Chaudret, P.J. Kooyman, F. Fajula, Microporous Mesoporous Mater. 79 (2005) 185–194.
[28] J. Zhu, Z. Konya, V.F. Puntes, I. Kiricsi, C.X. Miao, J.W. Ager, A.P. Alivisatos, G.A. Somorjai, Langmuir 19 (2003) 4396–4401.
[29] I. Yuranov, P. Moeckli, E. Suvorova, P. Buffat, L. Kiwi-Minsker, A. Renken, J. Mol. Catal. A: Chem. 192 (2003) 239–251.
[30] J.E. Hampsey, S. Arsenault, Q. Hu, Y. Lu, Chem. Mater. 17 (2005) 2475–2480.
[31] K.S. Morley, P. Licence, P.C. Marr, J.R. Hyde, P.D. Brown, R. Mokaya, Y. Xia, S.M. Howdle, J. Mater. Chem. 14 (2004) 1212–1217.
[32] S. Martínez, A. Vallribera, C.L. Cotet, M. Popovici, L. Martin, A. Roig, M. Moreno-Mañas, E. Molins, N. J. Chem. 29 (2005) 1342–1345.
[33] A. Papp, G. Galbács, Á. Molnár, Tetrahedron Lett. 46 (2005) 7725–7728.
[34] C.P. Mehert, D.W. Weaver, J.Y. Ying, J. Am. Chem. Soc. 120 (1998) 12289–12296.
[35] L. Li, J.L. Shi, J.N. Yan, Chem. Commun. (2004) 1990–1991.
[36] N. Kim, M.S. Kwon, C.M. Park, J. Park, Tetrahedron Lett. 45 (2004) 7057–7059.
[37] J.H. Clark, D.J. Macquarrie, E.B. Mubofu, Green Chem. 2 (2000) 53–55.
[38] E.B. Mubofu, J.H. Clark, D.J. Macquarrie, Green Chem. 3 (2001) 23–25.

[39] A.H.M. de Vries, J.M.C.A. Mulders, J.H.M. Mommers, H.J.W. Henderickx, J.G. de Vries, Org. Lett. 5 (2003) 3285–3288.
[40] M.T. Reetz, J.G. de Vries, Chem. Commun. (2004) 1559–1563.
[41] B.M. Choudary, S. Madhi, N.S. Chowdari, M.L. Kantam, B. Sreedhar, J. Am. Chem. Soc. 124 (2002) 14127–14136.
[42] K. Okamoto, R. Akiyama, H. Yoshida, T. oshida, S. Kobayashi, J. Am. Chem. Soc. 127 (2005) 2125–2135.
[43] Y.J. Jiang, Q.M. Gao, J. Am. Chem. Soc. 128 (2006) 716–717.
[44] K. Mori, T. Hara, T. Mizugaki, K. Ebitani, K. Kaneda, J. Am. Chem. Soc. 126 (2004) 10657–10666.
[45] D. Zhao, Q. Huo, J. Feng, B.F. Chmelka, G.D. Stucky, J. Am. Chem. Soc. 120 (1998) 6024–6036.